# The H.E.S.S. Extragalactic Sky

Jill Chevalier, Laboratoire d'Annecy-le-Vieux de Physique des Particules,
Université Savoie Mont-Blanc, CNRS/IN2P3, F-74941 Annecy-le-Vieux, France
for the H.E.S.S. Collaboration

February 28, 2016

**Abstract**

The High Energy Stereoscopic System (H.E.S.S.) is an array of 5 Imaging Atmospheric Cherenkov Telescopes located in the Khomas Highland, Namibia. The first four 12 meters dish telescopes have been operating since 2002 and a fifth telescope (with a 28m diameter dish) had been added to the array in 2012 improving the sensitivity towards lower energies. Highlights of recent results of H.E.S.S. on extragalactic studies observations will be presented, more especially on blazars (PKS 2155-304, Mrk 501, PG 1553+113), the extragalactic background light and an update on the H.E.S.S. Gamma-Ray Burst program.

## 1 Introduction

The High Energy Stereoscopic System (H.E.S.S.) Phase-I began in 2002 with 4 small 12-meters telescopes working in stereoscopic mode, giving an energy threshold $\sim 100$ GeV, a field of view $\sim 5°$ and an angular resolution $< 0.1°$. Since 2012, H.E.S.S. entered its Phase-II with the addition of a fifth telescope (CT5). This $28 \times 32$ meters telescope has a bigger collection area for the Cherenkov light, allowing to decrease the energy threshold of the full array to few tens of GeV. With two different types of telescopes, H.E.S.S. is the first hybrid array of Cherenkov telescopes in the world.

Since the beginning of the experiment, H.E.S.S. discovered more than 80 objects (Galactic and extragalactic) at very high energies (VHE). Concerning extragalactic observations, H.E.S.S. focuses mostly on active galactic nuclei (AGN), more especially on blazars, and on transient objects. Section 2 will give insights on the H.E.S.S. Phase-II scientific projects, followed by the first H.E.S.S. Phase-II results on AGN (see Section 3). Section 4 will focus on variability studies of two well known blazars, Markarian 501 and PKS 2155-304. Section 5 will present the last result on the first model-independent study of the extragalactic background light (EBL).

## 2 H.E.S.S. Phase-II

With a hybrid array, different configurations to observe the sky are available, implying different triggers and different analyses. CT5 can be used alone in Monoscopic mode giving the lowest energy threshold, this mode is well suited to detect GRBs and high redshift AGN together with the study of the EBL. Telescopes can observe together in Stereoscopic mode, giving the best sensitivity in the core energy range of the experiment, which is best to detect weak sources and do morphology studies.

The improved sensitivity of CT5 allows to study all time scales of variability and detect transient objects. Fig.1 shows the sensitivity of CT5 in Monoscopic mode compared to the *Fermi*-LAT sensitivity at comparable energies. At small time scales, from seconds to minutes, CT5 is more sensitive, up to 5 orders of magnitude, compared to *Fermi*-LAT, reaching the threshold to detect fast variability objects as gamma-ray bursts at tens of GeV, an energy range unreachable before.

## 2.1 The H.E.S.S. II GRB program

Gamma-ray bursts (GRBs) are among the most energetic, luminous and exotic events in the Universe. They may be created by the collapse of a massive star or by merger events. The study of GRBs adresses multiple science objectives:

- determine if GRBs can explain the ultra high energy cosmic rays (UHECR) origin;
- study and constrain VHE radiation process(es) along with the jet physics;
- study the $\gamma$-$\gamma$ attenuation caused by the EBL;
- test the Lorentz invariance violation.

However, up to now, no GRB has been detected at TeV energies, leaving their behavior at these energies unknown. The addition of CT5 to the H.E.S.S. array is a step towards the detection of GRBs at TeV energies [1].

GRBs are short events, to catch them the drive system has been improved allowing the telescope to repoint faster, doing 180° in 110 seconds [2]. To decrease again the repointing time, CT5 can go in reverse mode (negative zenith angles), contrary to the H.E.S.S.-I telescopes. Taking into account this mode, the repointing time is generally smaller than 2 minutes. It has been tested on real and fake GRB alerts, giving an average repointing time around 80 seconds (Fig.1 right).

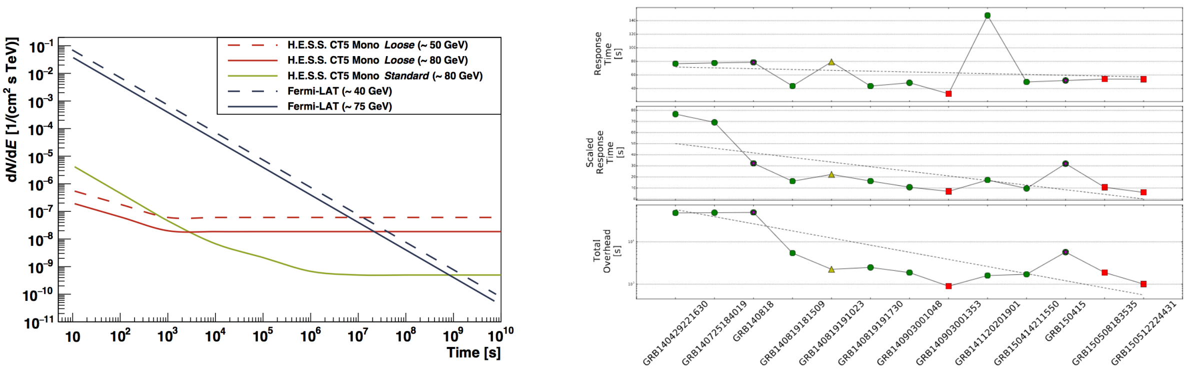


Figure 1: Left [3]: Sensitivity versus time of the H.E.S.S. CT5 telescopes in *Standard* (green) and *Loose* (red) cuts at $\sim$ 50 and $\sim$ 80 GeV compare to the sensitivity of the *Fermi*-LAT at $\sim$ 40 and $\sim$ 75 GeV (blue). Right [1]: (top) total response time; (middle) response time scale by the angular distance of the repointing; (bottom) data aquisition system time overhead for real and fake GRB observations.

The GRB alerts are received through the the Gamma-ray Coordinates Network (GCN)[1] by *Fermi*-GBM and *Swift*-BAT. This system is designed to send alert as fast as possible, with fewer number of hardware and software transitions in H.E.S.S., to minimise the repointing time.

## 2.2 Towards a population study at TeV

Up to now, $\sim$ 60 blazars have been discovered at VHE[2]. According to the current classification, blazars can be divided in 2 classes:

- Flat Spectrum Radio Quasars (FSRQ): highly luminous with strong emission lines;
- BL Lacartae (BL Lac): less luminous than FSRQs and with weak emission lines. This class is subdivided into low, intermediate and high frequency peak BL Lac (LBL, IBL, HBL) according to the frequency peak position of the synchrotron peak.

[1] The Gamma-ray Coordinates Network http://gcn.gscfc.nasa.gov
[2] according to the last numbers on TeVCat: http://tevcat.uchicago.edu/

Almost 80% of the TeV blazar sky are HBL, and it is not supposed to be representative of the real blazars population. There is an observational bias since VHE experiments focused on this type of objects on the first years because, following the blazar sequence [4], they are brighter in the TeV range. Currently, there are only 5 FSRQs, 1 LBL and 8 IBLs detected at VHE, which is not enough to probe the blazar sequence or perform a population study.

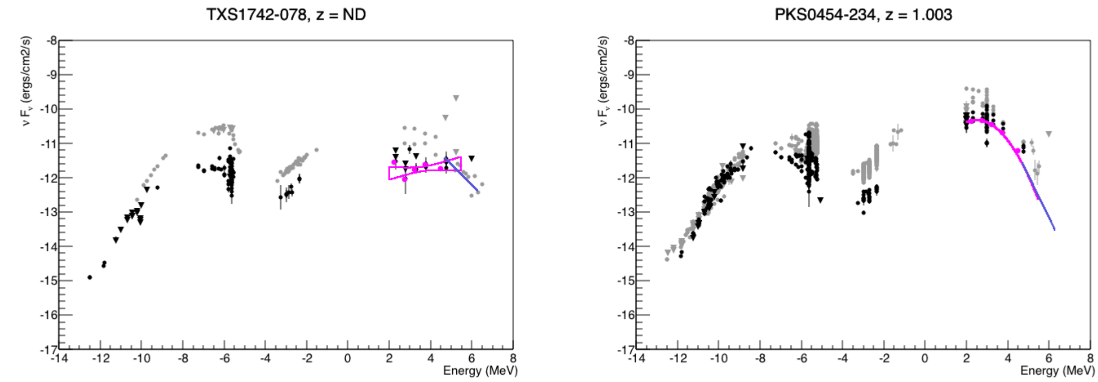


Figure 2: Left: Public SED data of LBL object TXS 1741-078 (black) together with 3FGL (pink) and 2FHL (blue) *Fermi* catalogs data (see [10] and [11]) compared to the MWL SED of Ap Librae (in grey). Right: Public SED data of LBL object PKS 0454-234 (black) together with 3FGL (pink) and 2FHL (blue) *Fermi* catalogs data compared to the MWL SED of PKS 1510-089 (grey).

Fig.2 shows the spectral energy distributions (SED) of TXS 1742-078 and PKS 0454-234, respectively LBL and FSRQ objects. These objects appear to be good TeV candidates when comparing their SEDs to the SED of already known TeV blazar like Ap Librae [5] or PKS 1510-089 [6].

Observations of few candidates will take place during the following years, and will hopefully lead to new discoveries which will complement the blazar sequence in the VHE range.

## 3 First H.E.S.S.-II AGN results

Two well known blazars, PKS 2155-304 (z = 0.116) and PG 1553+113 ($0.43 < z < 0.58$) were observed with a Monoscopic configuration respectively in 2013-2014 and 2013 [7]. The data were chosen following the standard run quality criteria and analyzed using the standard Model reconstruction described in [8] adapted for the Mono events [9].

PKS 2155-304 is well detected at $42\sigma$ in the full energy range. Below 100 GeV, the source is confidently detected at $10\sigma$ (Fig.3 top left) with a well controlled background. The H.E.S.S.-II spectrum is reconstructed with a conservative energy threshold of 80 GeV and is well described by a log-parabola with a photon index $\alpha = 2.63 \pm 0.07_{\mathrm{stat}}$ and a curvature $\beta = 0.24 \pm 0.06_{\mathrm{stat}}$ (Fig.3 top right).

PG 1553+113 is detected at high significance in the full energy range. Between 100 and 130 GeV, the source is confidently detected at $10\sigma$ (Fig.3 bottom left) with a well controlled background. The H.E.S.S.-II spectrum is reconstructed with a higher energy threshold of 100 GeV due to a higher zenith angle, and is well described by a log-parabola with a photon index $\alpha = 2.95 \pm 0.23_{\mathrm{stat}}$ and a curvature $\beta = 1.04 \pm 0.31_{\mathrm{stat}}$ (Fig.3 bottom right).

This new measurements agree with previous H.E.S.S. measurements along with the 3FGL and 1FHL *Fermi* catalog spectra (see [10] and [12]), proving the capability of CT5.

## 4 Variability studies in blazars

Blazars show variability across the entire electromagnetic spectrum at all time scales, from minutes to years. The current blazar paradigm states that the non-thermal emission is produced by relativistic jets, powered by a supermassive black hole fed by an accretion disk. Variability aims to study the

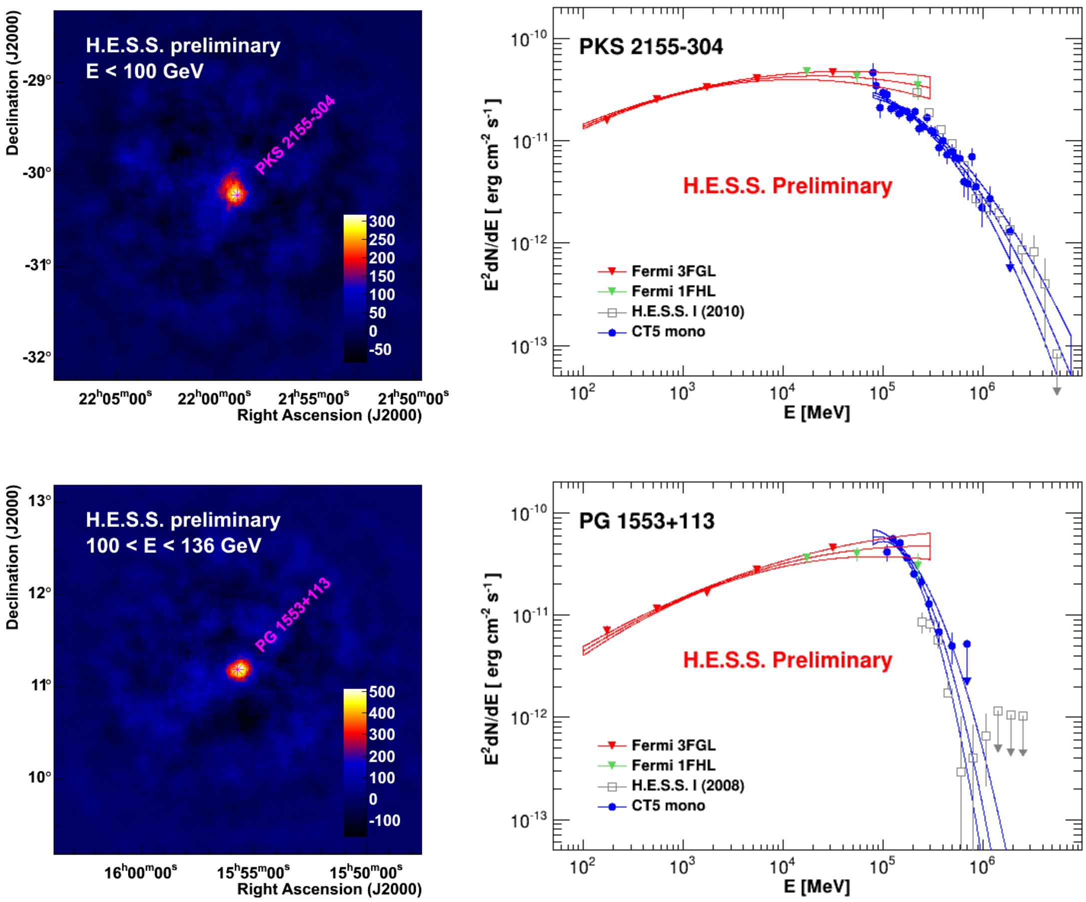


Figure 3: Top: excess map below 100 GeV and 3FGL (red), 1FHL (green) and H.E.S.S.-I (grey) and H.E.S.S.-II (blue) spectra of PKS 2155-304. Top: excess map between 100 and 130 GeV and 3FGL (red), 1FHL (green) and H.E.S.S.-I (grey) and H.E.S.S.-II (blue) spectra of PG 1553+113 [7].

physical conditions of this central engine together with the acceleration and emission processes, which are poorly known.

### 4.1 Short variability studies with Mrk 501 flare

The nearby blazar Mrk 501 (z = 0.034) has been observed during June 2014. During this observation period, a flare happened, triggering a ToO observation [13]. Due to the high zenith angle during observations, the energy threshold of the analysis is 2 TeV, allowing to study variability at purely TeV energies [14].

The statistic was high enough to separate the light curve in 4 minutes bins in different energy bins below and above 4.5 TeV, showing fast variability in all energy bins. The whole light curve of June 2014 shows a flux doubling time scale [15] $t_{\mathrm{doubling}} < 10$ minutes and a fractional root mean square variability [16] $F_{\mathrm{var}} = 1.1$ above 2 TeV. These value showing high and fast variability at TeV energies are flare-dominated.

The flux distribution gives hints about the emission mechanisms. Hence the flux and logarithm of the flux distributions were both fitted by a Gaussian. The latter is better fitted by a Gaussian than the first one, meaning that the flux follows a lognormal distribution. The process(es) seems to be multiplicative instead of additive. This is, in principle, characteristic of a cascade-like process, and has been found in other blazars like PKS 2155-304 at TeV during the 2006 flare [17] and BL Lacertae in X-ray [18].

### 4.2 Long term monitoring of the blazar PKS 2155-304

PKS 2155-304 is one of the brightest blazar of the southern sky which H.E.S.S. monitored every year, leading to more than 300 hours of data between 2004 and 2012 of observations. These data were used to study the long term variability of the blazar [19]. *Fermi*-LAT, *RXTE*, *Swift*-XRT, XMM-Newton and SMARTS data were also used to conduct a multi-wavelength study with the best coverage and simultaneity possible. In order to study the quiescent state of the blazar and to not be biased, all ToO observations were removed from the dataset (Fig.4).

The lognormality of the quiescent state has been investigated, looking at flux distributions and correlation between variability and flux. In all energy ranges, a preference is seen towards the lognormal behavior: the log flux distribution is better fitted by a Gaussian than the flux one and a clear correlation is seen between the excess rms $\sigma_{\rm XS}$ and the mean flux $\overline{\Phi}$ (the higher the flux the higher the amount of variability). This multiplicative behavior is seen with a significance $> 5\sigma$ for the TeV, X-ray and optical energy ranges and $\sim 2.6\sigma$ in the GeV range. Lognormality seems to be a intrinsic characteristic of PKS 2155-304.

The fractional root mean square variability [16] is another mean to look at variability. Its evolution with the energy is showed on Fig.5. $F_{\rm var}(E)$ is increasing throughout SED components, with a small variability in optical and GeV in contrast with a more pronounced variability in X-ray and TeV. The similar behavior of the variability at low (optical + X-ray) and high (GeV + TeV) energies might be a hint of the link between these two ranges in acceleration/emission process(es).

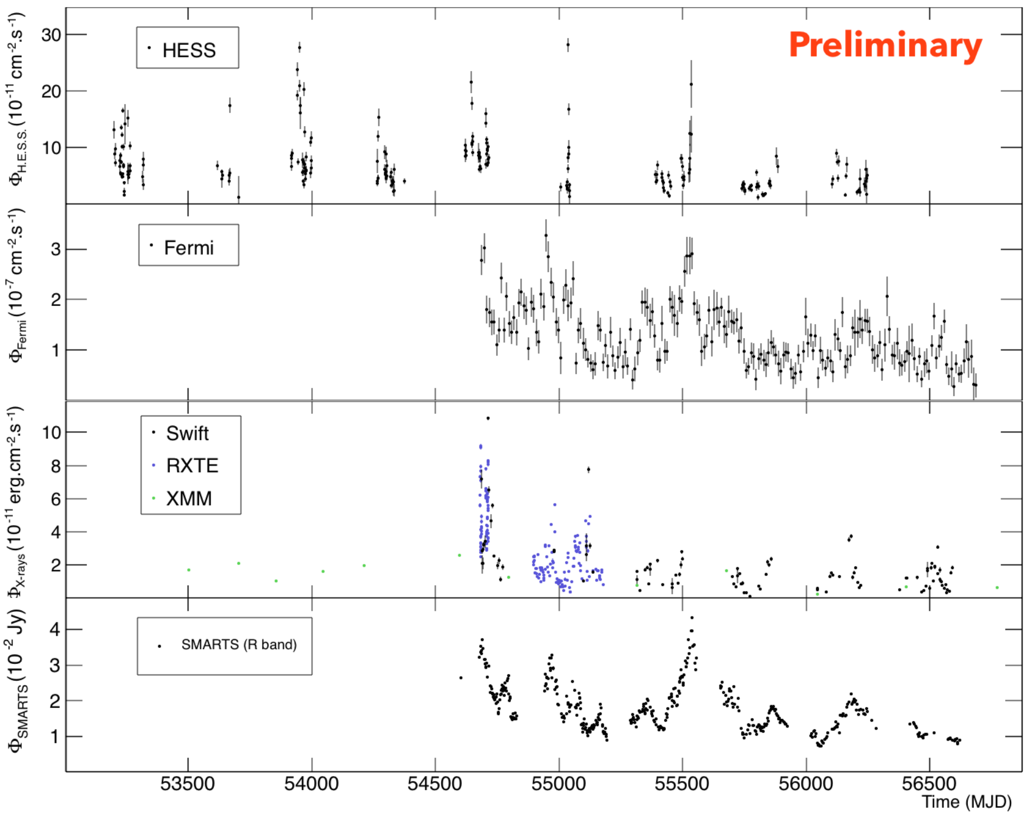


Figure 4: Multi-wavelength light curve of PKS 2155-304. From top to bottom: H.E.S.S. ($E > 200$ GeV) between 2004 and 2012, *Fermi*-LAT ($0.1 < E < 300$ GeV) between 2008 and 2013, X-rays with *Swift*-XRT, *RXTE* and XMM-Newton ($2 < E < 10$ keV) between 2004 and 2013, SMARTS (J, R, V, B bands) between 2008 and 2013.

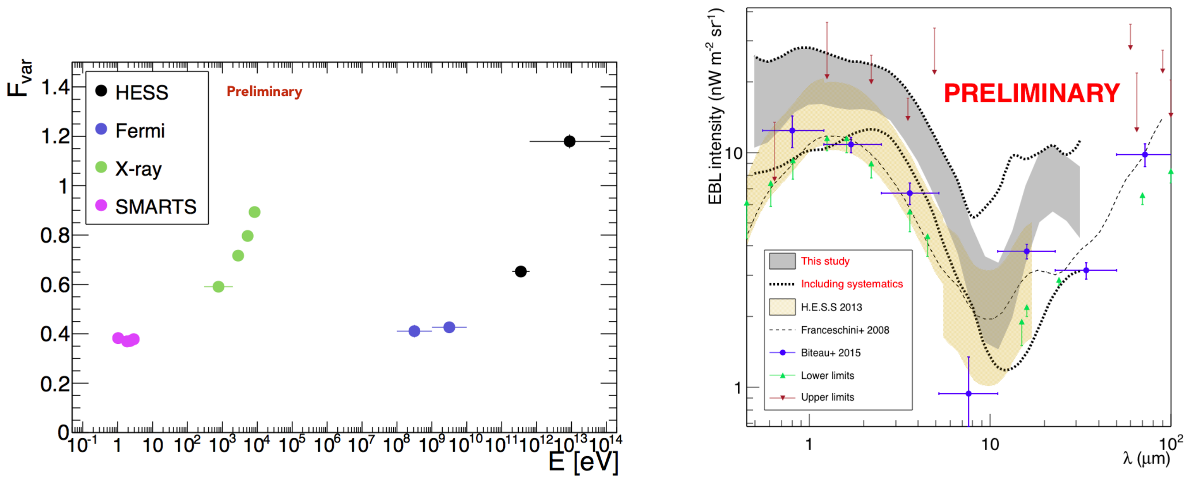


Figure 5: Left: Fractional root mean square variability energy profile of PKS 2155-304 with multi-wavelength data. Right: EBL shape and intensity with the last results from H.E.S.S. (grey) along with upper limits (red), lower limits (green), former results from [21] (blue) and the Franceschini model [22] (dashed black line).

## 5 Determining the EBL shape

The EBL is an isotropic and diffuse light (going from UV to far infrared) and consists of all the light emitted by stars and re-emitted by dust over the age of the Universe. It therefore encodes important cosmological parameters such as the star formation rate density. Because of the EBL, the Universe is not transparent to $\gamma$-rays over cosmological distances, hence $\gamma$-rays undergo electron-positron pair production with photons of the EBL. This interaction causes an exponential attenuation that scales with the optical depth $\tau$: $\Phi_{\rm obs}(E_\gamma) = \Phi_{\rm int}(E_\gamma) \times \exp(-\tau(E_\gamma, z))$. The difficulty in studying the EBL is to disentangle between intrinsic curvature and EBL absorption.

On Fig.5 (right) is the result of the first model-independent study of the EBL shape and intensity done with H.E.S.S. [20]. It uses a spline method to explore the EBL space, and accounts form upper limits from direct measurements and lower limits from galaxy counts. With the systematic errors, the new shape is consistent with the previous measurements.

## 6 Conclusion

Concerning blazars studies, there are 2 directions : (1) keep observing known blazars to study their long term variability as it has been done with PKS 2155-304 and trying to catch flares to study the short variability time scales at VHE; (2) detecting new objects, especially FSRQs and LBLs to probe the blazar sequence at TeV energies.

Studying the variability of blazar, either short or long term, helps to put constrains on emission and acceleration mechanisms and on the localisation on the emission region. Recent results show blazars tend to have a lognormal behavior, which is a signature of multiplicative processes, as shown for the long term monitoring of PKS 2155-304 and the 2014 flare of Mrk 501 along with other blazars (see [17] and [18]). Lognormal behavior has been seen for the first time in X-ray binaries [23] linking lognormality to accretion disks. Seeing a lognormal behavior also into blazars suggests that the accretion disk creates a lognormal variability which imprints itself on the jet afterwards. Moreover the variability profile $F_{\rm var}(E)$ will be a useful tool to disentangle between different acceleration and emission models.

Discovering more VHE emitters in the FSRQ and LBL subclasses will be a first step to have a better understanding of these objects and more generally of the acceleration and emission mechanisms at play in AGN along with the emission localisation region.

The Phase-II of the H.E.S.S. experiment is now fully operating. The addition of CT5 will hopefully leads to new discovery in the GRB and transient domains, thanks to a better sensitivity and an improved drive system. The analysis chains have been adapted to account for CT5 and are now working as shown with the first H.E.S.S.-II AGN results, the full paper with more details is currently in preparation.

## References

[1] Parsons, R. D., Balzer, A., Fssling, M., Hoischen, C., Holler, M., Mitchell, A. M. W., ... & O'Brien, P. (2015). The HESS II GRB Program. arXiv preprint arXiv:1509.05191.

[2] P. Hofverberg, R. Kankanyan, M. Panter, et al. Commissioning and initial performance of the H.E.S.S. II drive system. Proceedings of the 33rd International Cosmic Ray Conference, 2013.

[3] Holler, M., Balzer, A., Chalm-Calvet, R., de Naurois, M., & Zaborov, D. (2015). Photon reconstruction for HESS using a semi-analytical shower model. arXiv preprint arXiv:1509.02896.

[4] Fossati, G. A., Maraschi, L., Celotti, A., Comastri, A., & Ghisellini, G. (1998). A unifying view of the spectral energy distributions of blazars. Monthly Notices of the Royal Astronomical Society, 299(2), 433-448.

[5] Sanchez, D. A., Giebels, B., Fortin, P., Horan, D., Szostek, A., Fegan, S., ... & Lister, M. L. (2015). From radio to TeV: the surprising spectral energy distribution of AP Librae. Monthly Notices of the Royal Astronomical Society, 454(3), 3229-3239.

[6] Collaboration, H. E. S. S., Abramowski, A., Acero, F., Aharonian, F., Akhperjanian, A. G., Anton, G., ... & Tjus, J. B. (2013). HESS discovery of VHE gamma-rays from the quasar PKS 1510-089. arXiv preprint arXiv:1304.8071.

[7] Zaborov, D., Romoli, C., Taylor, A. M., Lenain, J. P., Sanchez, D., & Parsons, R. D. (2015). AGN observations with a less than 100 GeV threshold using HESS II. arXiv preprint arXiv:1509.06509.

[8] De Naurois, M., & Rolland, L. (2009). A high performance likelihood reconstruction of $\gamma$-rays for imaging atmospheric Cherenkov telescopes. Astroparticle Physics, 32(5), 231-252.

[9] Holler, M., Balzer, A., Chalm-Calvet, R., de Naurois, M., & Zaborov, D. (2015). Photon reconstruction for HESS using a semi-analytical shower model. arXiv preprint arXiv:1509.02896.

[10] Acero, F., Ackermann, M., Ajello, M., Albert, A., Atwood, W. B., Axelsson, M., ... & Belfiore, A. (2015). Fermi large area telescope third source catalog. The Astrophysical Journal Supplement Series, 218(2), 23.

[11] Collaboration, T. F. L. (2015). 2FHL: The Second Catalog of Hard Fermi-LAT Sources. arXiv preprint arXiv:1508.04449.

[12] Ackermann, M., Ajello, M., Allafort, A., Atwood, W. B., Baldini, L., Ballet, J., ... & Bellazzini, R. (2013). The first Fermi-LAT catalog of sources above 10 GeV. The Astrophysical Journal Supplement Series, 209(2), 34.

[13] Stegmann, C. (2014). Increased VHE activity from Mrk 501 detected with HESS. The Astronomer's Telegram, 6268, 1.

[14] Chakraborty, N., Cologna, G., Kastendieck, M. A., Rieger, F., Romoli, C., Wagner, S. J., ... & Taylor, A. (2015). Rapid variability at very high energies in Mrk 501. arXiv preprint arXiv:1509.04893.

[15] Y. H. Zhang and C. M. Celotti, A. and...Urry, Rapid X-Ray Variability of the BL Lacertae Object PKS 2155-304, ApJ 527 (Dec., 1999) 719−732, [astro-ph/9907325].

[16] S. Vaughan, R. Edelson, R. S. Warwick, and P. Uttley, On characterizing the variability properties of X-ray light curves from active galaxies, MNRAS 345 (Nov., 2003) 1271-1284, [astro-ph/0307420].

[17] H.E.S.S. Collaboration and H. S. Abramowski, A. and..Zechlin, VHE $\gamma$-ray emission of PKS 2155-304: spectral and temporal variability, A&A 520 (Sept., 2010) A83, [arXiv:1005.3702].

[18] Giebels, B., & Degrange, B. (2009). Lognormal variability in BL Lacertae. Astronomy & Astrophysics, 503(3), 797-799.

[19] Chevalier, J., Kastendieck, M. A., Rieger, F., Maurin, G., Lenain, J. P., & Lamanna, G. (2015). Long term variability of the blazar PKS 2155-304. arXiv preprint arXiv:1509.03104.

[20] Lorentz, M., Brun, P., & Sanchez, D. (2015). Determination of the extragalactic background light spectral energy distribution with HESS. arXiv preprint arXiv:1509.03477.

[21] H.E.S.S Collaboration (2013). Measurement of the extragalactic background light imprint on the spectra of the brightest blazars observed with HESS. Astronomy & Astrophysics, 550, A4

[22] Franceschini, A., Rodighiero, G., & Vaccari, M. (2008). Extragalactic optical-infrared background radiation, its time evolution and the cosmic photon-photon opacity. Astronomy & Astrophysics, 487(3), 837-852.

[23] Uttley, P., & McHardy, I. M. (2001). The flux-dependent amplitude of broadband noise variability in X-ray binaries and active galaxies. Monthly Notices of the Royal Astronomical Society, 323(2), L26-L30.